geoconvention
Virtual Event September 13 - 15 2021

Processing to inversion: a case study of revitalizing legacy seismic data offshore Nova Scotia

Natasha Morrison[1], Abhishek Raj[2], Elena Dutcher[2], Cody Evans[2], Sagnik Dasgupta[2], Edan Gofer[2], Keith Nunn[3] and Matt Luheshi[4]

[1]Nova Scotia Department of Energy and Mines; [2]Schlumberger; [3]NunnGeo Consulting Ltd; [4] Leptis E&P Ltd.

Summary

The reprocessing and analysis of legacy datasets has become the economic alternative to acquiring new data. The Nova Scotia Department of Energy and Mines has undergone a project with Schlumberger to reprocess the Barrington narrow-azimuth, 3D surface seismic survey. Acquired in 2001, the survey covers an area of approximately 1800 km^2 located over the outer shelf and slope of the southwestern Scotian Basin (Figure 1). Deptuck et al. (2015) have identified potential prospectivity in the form of amplitude anomalies in Cretaceous turbidite channels and shallower Tertiary sediments.

For the reimaging, through the use of contemporary processing techniques such as broadband processing and high-resolution tomography, the 3D survey was reprocessed to a full tilted transverse isotropy Kirchhoff prestack depth migration from the legacy isotropic Kirchhoff time migration. In addition to this reprocessing, an ongoing rock physics and AVO study was conducted with this updated data.

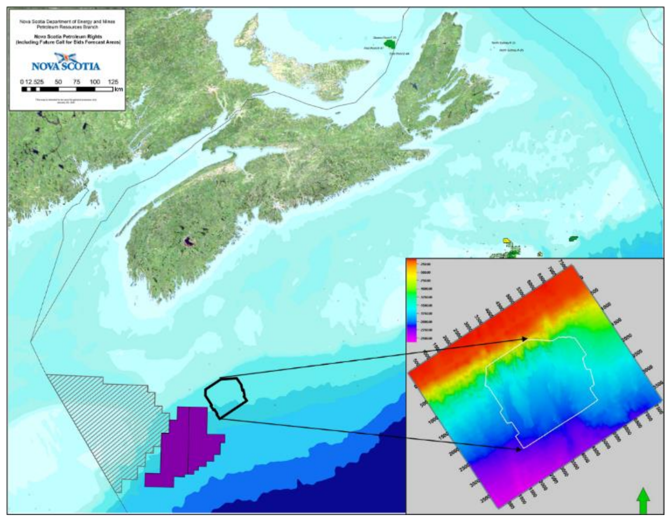

Figure 1: Location of the Barrington 3D in offshore, Nova Scotia with Barrington Seafloor inset.

Workflow

The reprocessing workflow on the Barrington 3D dataset was tailored to include modern processing techniques such as adaptive deghosting, true-azimuth multiple elimination and matching pursuit Fourier interpolation. Combined with high resolution tilted transverse isotropy (TTI) modeling and migration, the data were processed to full AVO compliance. A velocity profile from a legacy 2D seismic line was used to initialize the velocity model in the absence of the original Kirchhoff prestack time migration (PSTM) 3D velocity model and lack of well data within the seismic extents. Gathers created in this process will be used for litho-elastic AVO inversion (Bachrach and Gofer, 2020). There are no wells with geophysical logs within the survey area; therefore, elastic parameter trends meant to be used in the inversion are derived from deterministic and stochastic rock physics modeling (Avseth et al., 2010; Bachrach, 2011).

This project utilized broadband seismic signal processing sequences, as the extended bandwidth provides a significant uplift in interpretation and inversion. The first step was a data-dependent noise attenuation workflow (Espinoza et al., 2019), applied to attenuate most of the low-frequency noise. Data were then processed through a series of coherent and random noise attenuation modules to increase the signal-to-noise ratio. The adaptive deghosting algorithm (Rickett et al., 2014) was used for source and receiver deghosting. This approach performs debubble, deghosting and zero phasing simultaneously with the use of source wavelet (Caprioli et al., 2019). Figure 2 depicts the shot gather and stack comparison before and after deghosting. Figure 2(c) and 2(f) shows the zero phased water bottom wavelet and amplitude spectrum comparison respectively. The attenuated high-frequency signal was recovered through application of post migration Q-amplitude compensation.

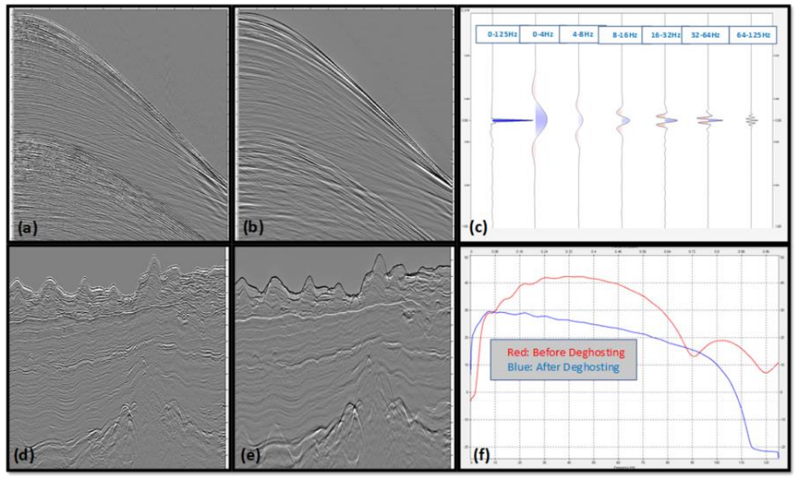

Figure 2:(a) Shot Gather before deghosting, (b) shot gather after deghosting, (c) WB wavelet and its filter panels, (d) stack before deghosting, (e) stack after deghosting and (f) amplitude spectrum comparison for the stack shown in (d) And (e).

A series of demultiple workflows was designed to attenuate multiples after the deghosting workflow, with most modeled using a true azimuth surface-related multiple-elimination algorithm (Moore and Dragoset, 2008). Post demultiple, data were interpolated and regularized to a finer grid (12.5mX18.75m) to increase the spatial resolution. The matching pursuits Fourier interpolation (MPFI) algorithm (Schonewille et al., 2009) used for this purpose also filled the acquisition holes in each offset bin and improved the signal-to-noise ratio.

After combining the legacy single-function velocity profile with regionally interpreted horizons, a smooth 3D velocity field was obtained. The velocity field was updated in a geologically consistent manner by using five iterations of high-resolution multi-scale common image point (CIP) tomography (Woodward et al, 2008). At right in Figure 3, velocity variations along the salt-bounded mini-basin are propagated even along the steepest dips. The salt interpretation shown in this image

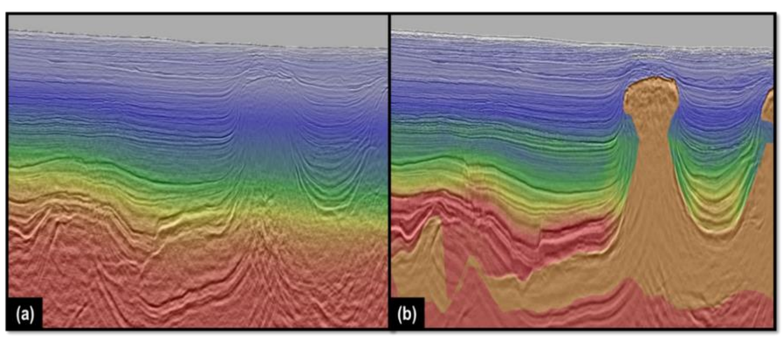

Figure 3:a) Single function initial p-velocity overlain on corresponding Kirchhoff Depth Migration (KDM) stack compared to b) final p-velocity overlain on corresponding KDM stack. 3:1 vertical exaggeration used to emphasize high-resolution detail.

was generated through a series of flood and body migrations for encapsulating both allochthonous and autochthonous salt features, with an observed clean velocity of 4500 m/s.

Observations

The new Kirchhoff prestack depth migration (KPSDM) clearly shows enhanced stratigraphy, salt body definition, and more detailed structural imaging. Faults, short-wavelength folds, and previously unidentified gas bodies are also accurately imaged. Improved imaging, seen in Figure 4, has provided further refinement and understanding of original play concepts, such as the Cayuga prospect identified by Deptuck et al. in 2015. Initial scanning of AVO gradient sections (0-30°) of the final gathers show an interpreted gas sand anomaly at 5.5s within the Jurassic giving some support for charge from a Lower Jurassic source (Figure 5).

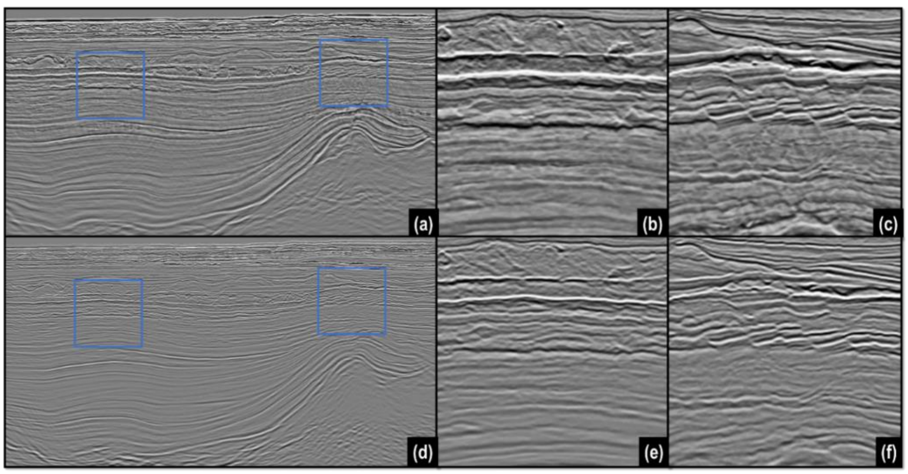

Figure 4: a) Reprocessing TTI KPSDM with b) left zoom section and c) right zoom section, compared to the d) legacy isotropic KPSTM stack with e) left zoom section and f) right zoom section. KPSDM stack stretched from depth to time for comparison.

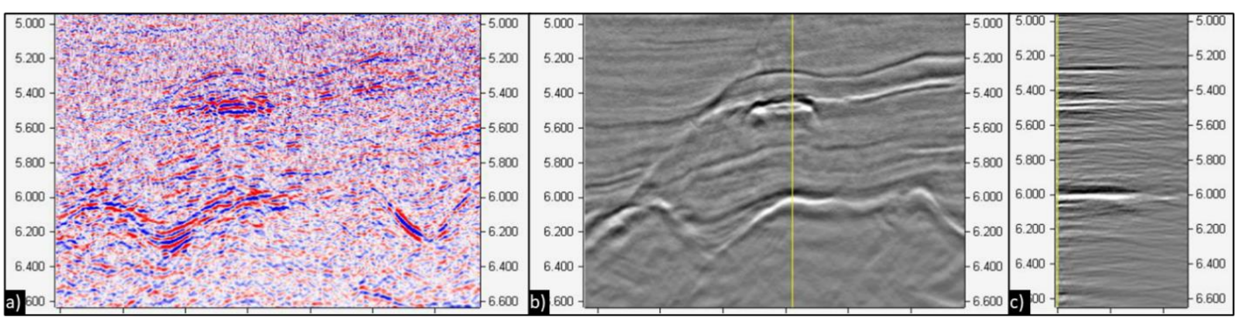

Figure 5: a) AVO Gradient with amplitude anomaly at appx. 5.5s b) Reprocessing TTI KPSDM stack stretched from depth to time c) Gathers corresponding to yellow line in b.

In addition, rock physics modeling undertaken on nearby wells clearly show a strong dependence of shale trends on effective stress and temperature. Figure 6 shows the impact of temperature and effective stress on the transition from smectite to illite clay. This dependency has a strong impact on acoustic impedance and Vp/Vs for the key rock classes analyzed in this study (sand, shale, and carbonate). The rock physics models formed the a priori information that will be used as input to the litho-elastic inversion. The resulting lithology and probability cubes from the inversion will refine the evaluation of the prospectivity in the area.

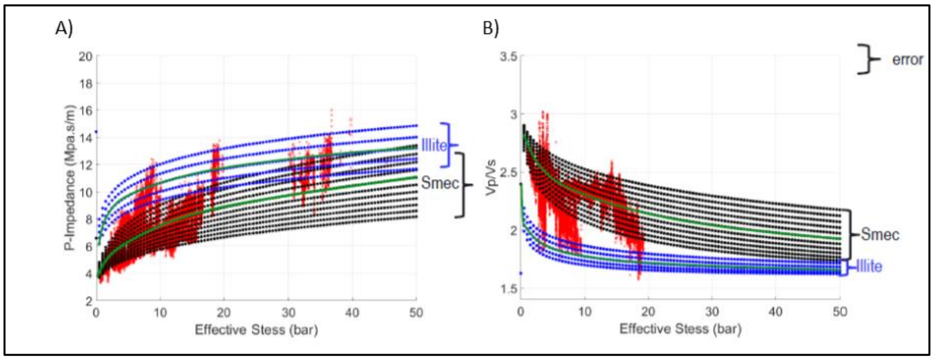

Figure 6: Inversion attributes from the stochastic rock physics illustrating two shale trends A) Effective Stress vs AI B) Vp/Vs vs effective stress modeling (Black: temperature below 1105° C - mostly smectite; Blue: temperature above 125° C - mostly illite).

Acknowledgements

The authors would like to acknowledge and thank Romualdo Pascoal, Hugo Enrique Munoz Cuenca and Ran Bachrach (Schlumberger) and Mark Deptuck (CNSOPB) for their contributions to this project.

References

Avseth, P., Mukerji, T., Mavko G., and Dvorkin, J., 2010, Rock-physics diagnostics of depositional texture, diagenetic alteration, and reservoir heterogeneity in high-porosity siliciclastic sediments and rock - a review of selected model and suggested workflow: GEOPHYSICS, 75, 5, 75A31 – 75A47.

Bachrach, R., 2011, Elastic and resistivity anisotropy in shale during compaction and diagenesis: Joint effective medium modeling and field observation: GEOPHYSICS, 76, 7, E175 – E186.

Bachrach, R., and Gofer, E., 2020, A nonlinear and anisotropic data-driven litho-petroelastic inversion for single-loop subsurface characterization: Theory, uncertainties, and a case study: The Leading Edge, 39, 2, 119 – 127.

Caprioli, P., Roth, J., Rickett J., and Vassallo M., 2019, Joint Adaptive Deghosting and Designature, 81st EAGE Conference and Exhibition,DOI: 10.3997/2214-4609.201900850

Deptuck, M, Brown, D and Altheim, B, 2015, Call for Bids NS15-1 –Exploration history, geologic setting, and exploration potential: Western and Central regions: Canada-Nova Scotia Offshore Petroleum Board. Available from https://callforbids.cnsopb.ns.ca/2015/01/sites/default/files/inline-pdf/deptuck_et_al_ western_and_central_regions052815.pdf

Espinoza, C., Vassallo, M., Nichols, D., Ray, M., and Yan, Z., (2019), Cross-Flow Noise Attenuation and Imaging of UltraLow Frequencies in Multivessel Circular Shooting Acquisition Surveys, Volume 2019, p.1 – 5, https://doi.org/10.3997/2214-4609.201900841

Moore, I., and B. Dragoset, 2008, General surface multiple prediction: A flexible 3DSRME algorithm: First Break, 26, 89–100.

Rickett, J., Van Manen D.-J., Loganathan P., and Seymour N., (2014), Slanted-streamer data-adaptive de-ghosting with local plane waves: 76th EAGE Conference and Exhibition, Extended Abstracts DOI: 10.3997/2214-4609.20141453

Schonewille, M., Klaedtke, A., Vigner. A., John Brittan.,and Martin, T., 2009, Seismic data regularization with the anti-alias anti-leakage Fourier transform: The First Break,27, 85-92.

Woodward, Marta & Nichols, Dave & Zdraveva, Olga & Whitfield, Phil & Johns, Tony. (2008). A decade of tomography. Geophysics. 73. 10.1190/1.2969907.